MicroRNA-21 targets the vitamin D-dependent antimicrobial pathway in leprosy

Philip T. Liu[1,2], **Matthew Wheelwright**[2], **Rosane Teles**[2], **Evangelia Komisopoulou**[3], **Kristina Edfeldt**[2], **Benjamin Ferguson**[2], **Manali D. Mehta**[4], **Aria Vazirnia**[4], **Thomas H. Rea**[5], **Euzenir N. Sarno**[6], **Thomas G. Graeber**[3], and **Robert L. Modlin**[2,4]

[1]Orthopaedic Hospital Research Center, University of California at Los Angeles, CA 90095, USA

[2]Division of Dermatology, Department of Medicine, David Geffen School of Medicine at University of California at Los Angeles, CA 90095, USA

[3]Crump Institute for Molecular Imaging, Institute for Molecular Medicine, Jonsson Comprehensive Cancer Center, California NanoSystems Institute, Department of Molecular and Medical Pharmacology, University of California, Los Angeles, CA 90095, USA

[4]Department of Microbiology, Immunology and Molecular Genetics, at University of California at Los Angeles, CA 90095, USA

[5]Department of Dermatology, University of Southern California School of Medicine, Los Angeles, CA

[6]Leprosy Laboratory Institute Oswaldo Cruz, Rio de Janeiro, Brazil

Abstract

Leprosy provides a model to investigate mechanisms of immune regulation in humans, given that the disease forms a clinical-immunological spectrum. Here, we identified 13 miRNAs that were differentially expressed in the lesions of subjects with progressive lepromatous (L-lep) vs. the self-limited tuberculoid (T-lep) disease. Bioinformatic analysis revealed a significant enrichment of L-lep-specific miRNAs that preferentially target key immune genes downregulated in L-lep vs. T-lep lesions. The most differentially expressed miRNA in L-lep lesions, hsa-mir-21, was upregulated in *M. leprae*-infected monocytes. Hsa-mir-21, by downregulating toll-like receptor 2/1 (TLR2/1)-induced *CYP27B1* and *IL1B* as well as upregulating IL-10, inhibited gene expression of the vitamin D-dependent antimicrobial peptides, *CAMP* and *DEFB4A*. Conversely, knockdown of hsa-mir-21 in *M. leprae*-infected monocytes enhanced expression of *CAMP* and *DEFB4A* and restored TLR2/1-mediated antimicrobial activity against *M. leprae*. Therefore, the ability of *M. leprae* to upregulate hsa-mir-21 targets multiple genes associated with the immunologically localized disease form, providing an effective mechanism to escape from the vitamin D-dependent antimicrobial pathway.

Address correspondence and reprint requests to: Dr. Philip T. Liu, Phone: (310) 206-8457, ptliu@mednet.ucla.edu.

Interactions between the host immune response and the invading pathogen at the site of disease are critical to the outcome of the infection. Leprosy, caused by the intracellular bacterium *Mycobacterium leprae*, provides an extraordinary model for studying host-pathogen interactions in humans. The disease presents as a spectrum where the clinical manifestations correlates with the level of immune response to the pathogen [1], which contributes to host defense vs. persistence and pathogenesis. At one end of the spectrum, the tuberculoid form (T-lep), the infection is self-limited, where skin lesions are typified by an adaptive immune response characterized by Th1 cytokines [2, 3] and an innate immune response characterized by macrophages programmed to express the vitamin D-mediated antimicrobial pathway [4]. At the other end of the spectrum, the lepromatous form (L-lep), the infection is disseminated with lesions typified by an adaptive immune response characterized by Th2 cytokines [2, 3] and an innate immune response characterized by macrophages programmed to express a phagocytic activity [4]. In order to gain insight into the mechanism(s) that regulate host defense vs. persistence in human infectious disease, we investigated miRNA expression in leprosy skin lesions.

Results

Gene and miRNA prolife in leprosy

The mRNA and miRNA expression profiles in skin lesions were determined in biopsy specimens from six T-lep and five L-lep patients collected at the time of diagnosis and classified according to the clinical and histopathological criteria of Ridley (Supplemental Fig. 1) [1]. Unsupervised hierarchal clustering analysis of the mRNA profiles revealed two major groups in which the L-lep and T-lep samples were segregated (Supplemental Fig. 2). In contrast, hierarchal clustering analysis of the miRNA profiles performed on the same samples indicated two major miRNA patterns, with each group containing a mixture of both L-lep and T-lep samples (Supplemental Fig. 2). These results indicate that the principal component of the measured miRNA expression patterns in leprosy did not differentiate the lesions types.

In order to identify lesion-specific differences we used a supervised approach. Differentially expressed miRNAs between the two clinical groups were identified by ranking miRNAs probes according to statistically significance (t-test) and limited to sequences present in the miRBase database (version 14). There was a five-fold greater number of differentially expressed miRNAs in the L-lep samples (16 probes representing 13 annotated miRNA species) vs. the T-lep samples (three probes representing two unique miRNA species) (Fig. 1a). In order to compare the magnitude of differential expression between these miRNA species, the un-normalized intensity values of the probes were compared. The difference in intensity of the hsa-mir-21 probe was the greatest of the miRNA species differentially upregulated in L-lep vs. T-lep lesions (Fig. 1b).

Targeting of immune genes by leprosy specific miRNAs

Because the differentially expressed miRNA species were predominantly enriched in L-lep lesions, we hypothesized that regulation of miRNA expression at the site of the progressive disease inhibits expression of genes involved in host defense against the pathogen. This

hypothesis was tested by integrating a prediction algorithm for miRNA binding sites in the three prime untranslated regions (3′UTR) of messenger RNA species with curated sets of host immune response signature genes known to be differentially expressed in leprosy lesions, including Th1 vs. Th2 related genes as well as the genes of the vitamin D pathway (Supplemental Text). All miRNA species represented on the microarray platform were ranked by their 'targeting preference score', calculated as the difference in frequency for targeting of the T-lep compared to L-lep signature genes (Supplemental Fig. 3 and Text). Enrichment analysis of leprosy disease-type specific miRNA species was next evaluated by the Kolmogorov-Smirnov-based permutation test. The L-lep-specific miRNA species were found to be significantly associated with the miRNAs most strongly predicted to preferentially target T-lep signature genes ($P = 0.049$; Fig. 1c). Thus, L-lep-specific miRNAs provide a candidate mechanism for the leprosy-induced downregulation of T-lep host immune response signature genes in L-lep lesions.

In relation to the local immune response, the L-lep specific set of miRNA species were predicted to have binding sites in the 3′UTR of Th1-related signature genes, known to be differentially expressed in T-lep vs. L-lep lesions, with an average targeting frequency of 11.5%. In contrast, the L-lep specific set of miRNAs species demonstrated a significantly ($P = 0.0003$) lower frequency for Th2-related genes, known to be differentially expressed in L-lep vs. T-lep lesions, with an average targeting frequency of 1.3% (Fig. 1d). Strikingly, multiple L-lep specific miRNA species targeted two key genes in the vitamin D-dependent antimicrobial pathway, cytochrome P450, family 27, subfamily B, polypeptide 1 (*CYP27B1*) and interleukin 1, beta (*IL1B*), but not the antimicrobial peptides that are induced by this pathway, cathelicidin (LL-37 encoded by *CAMP*) and defensin, beta 4A (*DEFB4A*) [5, 6] (Fig. 1e). Taken together, these results indicate that the L-lep specific miRNAs target and potentially downregulate host defense genes in leprosy.

Regulation of hsa-mir-21 in leprosy

The tissue expression of the most differentially expressed miRNA, hsa-mir-21, in L-lep lesions was verified by real time PCR (qPCR) and fluorescent *in situ* hybridization (FISH) in additional leprosy tissue sections. By qPCR, hsa-mir-21 levels were significantly higher (3.5 fold, $P = 0.01$) in 10 L-lep vs. 11 T-lep lesions (Fig. 2a). An unrelated miRNA, hsa-let-7c, that was not differentially expressed in disease lesions by microarray analysis, was expressed at similar levels between the L-lep and T-lep lesions (Fig. 2b). Although the skin biopsies are comprised predominately of granulomas in the dermis, we could not rule out that the differential expression of hsa-mir-21 was due to non-immune cells. Therefore, using FISH we determined that the frequency of hsa-mir-21 positive cells in the granulomatous regions was 25-fold greater in the L-lep lesions vs. the T-lep lesions (98% vs.4% of nucleated cells, $P = 0.001$) (Fig. 2c). In the L-lep lesions, the hsa-mir-21 positive cells were located within the granulomas, in the same microanatomic locations as *M. leprae* (Fig. 2d). It was not possible to determine the frequency of cells expressing hsa-mir-21 and containing *M. leprae* as these are found in distinct subcellular compartments: microRNAs are located in the cytoplasm and the pathogen resides within phagosomes. A scrambled probe was used as a negative control to demonstrate the absence of non-specific binding in either lesion type (Supplemental Fig. 4a), and the positive control probe for the U6 non-coding small nuclear

RNA, demonstrated equivalent RNA integrity (Supplemental Fig. 4b). Taken together, these three approaches, microarray, qPCR and FISH, provide convincing evidence for the differential expression of hsa-mir-21 in L-lep vs. T-lep lesions.

Given that *M. leprae* and hsa-mir-21 were both identified in the granulomas, we hypothesized that *M. leprae* induced hsa-mir-21 expression in monocytes/macrophages, the predominant cell type in a granuloma and the primary cell infected by the pathogen. Human peripheral blood monocytes were infected with live *M. leprae* at different multiplicities of infection (MOI) for 18 and 40 h, and hsa-mir-21 levels measured by qPCR. Infection of monocytes with *M. leprae* triggered an upregulation of hsa-mir-21 in a dose-dependent and time-responsive manner, with a 4.1-fold change (*P* = 0.005) at 18 h, and 7.6-fold change (*P* = 0.00003) at 40 h, both at a MOI of 10 (Fig. 3a). In contrast, *M. leprae* infection of monocytes did not result in detectable upregulation of hsa-let-7c, (Fig. 3b).

To explore the mechanism by which *M. leprae* infection induces hsa-mir-21, the ability of several key cell wall biomolecules to trigger hsa-mir-21 was compared. Treatment of monocytes with phenolic glycolipid-I (PGL-I) induced a 2.9-fold change in hsa-mir-21 expression, whereas the *M. leprae* lipoarabinomman (LAM) and lipomannan (LM), as well as a synthetic triacylated lipopeptide (a toll-like receptor 2/1 ligand, TLR2/1L) did not significantly induce hsa-mir-21 (Fig. 3c). Together, these data demonstrate i) hsa-mir-21 is present at the site of disease in leprosy, ii) is associated with the progressive and disseminated form (L-lep) of the disease, iii) is specifically induced in monocytes by *M. leprae* infection; and iv) is triggered by an *M. leprae* specific glycolipid, PGL-I. It is therefore likely that *M. leprae* infection of macrophages induces the upregulation of hsa-mir-21 at the site of infection.

Regulation of the vitamin D pathway by hsa-mir-21

It was noteworthy that of all the L-lep specific miRNAs, only hsa-mir-21 had the potential to target both *IL1B* and *CYP27B1* (Fig. 1e), both required for TLR-induced, vitamin D-dependent expression of *CAMP* and *DEFB4A*, which encode antimicrobial peptides [5, 6]. The ability of hsa-mir-21 to regulate the expression of these antimicrobial genes was investigated by transfecting primary human monocytes with either the mature hsa-mir-21 oligo or a non-targeting control oligo, followed by activation using the TLR2/1L. As a control for targeting specificity, we determined that overexpression of hsa-mir-21 downregulated IFN-γ induced interleukin 12A (*IL12A*) mRNA, a direct target (Supplemental Fig. 5 and Ref 7). The presence of hsa-mir-21 during TLR2/1L activation of monocytes resulted in the downregulation of *IL1B* mRNA by 24% (*P* = 0.006, representative experiment Fig. 4a and averaged Fig. 4b). Despite the absence of predicted hsa-mir-21 target sites in the 3′UTR of interleukin 10 (*IL10*), transfection of hsa-mir-21 enhanced toll-like receptor 2/1 (TLR2/1)-induced *IL10* mRNA levels by 110% (*P* = 0.035, Figs. 4a and 4c), consistent with studies in murine cells [8]. In contrast, *IL6*, another cytokine without hsa-mir-21 target sequences, was not affected (Figs. 4a and 4c). TLR2/1-induced IL-1β secretion was reduced by 45% (*P* = 0.003), IL-10 release was enhanced by 85% (*P* = 0.001), and IL-6 levels did not change (representative experiment Supplemental Fig. 6 and averaged Fig. 4c). Therefore, the effect of hsa-mir-21 on TLR2/1-induced cytokine mRNAs and secreted proteins were consistent.

Transfection of hsa-mir-21 also resulted in a 34% decrease in TLR-induced expression of CYP27B1 (P = 0.008, Figs. 4a and b). Given that hsa-mir-21 downregulated TLR2/1-induced IL1B and CYP27B1, the effect of hsa-mir-21 on TLR2/1-induced antimicrobial peptide gene expression was examined. Strikingly, TLR2/1L induction of *CAMP* and *DEFB4A* mRNAs was significantly inhibited by transfection of hsa-mir-21, by 73% (P = 0.005) and 60% (P = 0.006) respectively (Figs. 4a and 4b). Given that hsa-mir-21 upregulated IL-10, the effect of rIL-10 on TLR-induced gene expression was investigated. The addition of rIL-10 inhibited TLR-induced *CAMP* by 26% and *DEFB4A* by 35%, whereas the inhibition of interleukin 12B (*IL12B*) was 76% (Supplemental Figs. 7a and 7b). Therefore, hsa-mir-21 enhancement of IL-10 induction may partially contribute to the inhibition of antimicrobial gene expression.

The direct binding of hsa-mir-21 to the TLR-induced, vitamin D dependent antimicrobial pathway genes was assessed using a 3′UTR reporter assay. Hsa-mir-21 was determined to directly bind the 3′UTR of both *CYP27B1* and *IL1B*, but did not bind to the 3′UTR of either *CAMP* or *DEFB4A* (Fig. 4d, Supplemental Fig. 8 and Supplemental Text). These data indicate that hsa-mir-21 inhibits TLR2/1-mediated *CAMP* and *DEFB4A* expression by directly regulating key epigenetic targets including *CYP27B1* and *IL1B*, as well as indirectly through induction of immune modulatory cytokine IL-10.

Role of hsa-mir-21 in the response to infection

Given the ability of hsa-mir-21 to downregulate key genes in the TLR-induced antimicrobial pathway, and the observation that *M. leprae* induced hsa-mir-21 in monocytes, we investigated whether hsa-mir-21 contributes to inhibition of the innate immune response during *M. leprae* infection. This was accomplished by transfecting monocytes with a hsa-mir-21 specific antisense oligo (αmir-21). Transfected monocytes were infected with live *M. leprae* [9] for 18 h, and then mRNA expression was measured. Presence of αmir-21 vs. a control oligo (αmir-neg), followed by *M. leprae* infection resulted in a significant reduction of hsa-mir-21 levels by 70% (P = 0.00002, Supplemental Figs. 9a and 9c). Consistent with the hsa-mir-21 overexpression experiment, the αmir-21 enhanced *IL12A* mRNA expression in the *M. leprae* infected monocytes (P = 0.006, Supplemental Figs. 9b and 9c).

Relevant to the vitamin D-dependent innate immune pathway, αmir-21 increased IL1B mRNA expression in the *M. leprae* infected monocytes by 118% (P = 0.047, Figs. 5a and 5b). In contrast, *IL10* mRNA was downregulated by 34% (P = 0.045) and there was no significant change in *IL6* mRNA levels (Figs. 5a and 5b). Importantly, knockdown of hsa-mir-21 resulted in the significant increase of *CYP27B1* (59%, P = 0.014), *CAMP* (100%, P = 0.0006), and *DEFB4A* (227%, P = 0.014) (Figs. 5a and 5b). These results provide evidence that the monocyte/macrophage can detect *M. leprae* infection and trigger the vitamin D-dependent antimicrobial pathway; however, this response is inhibited by the ability of the pathogen to upregulate hsa-mir-21.

Effects of hsa-mir-21 on innate antimicrobial activity

The role of hsa-mir-21 in regulating the TLR2/1-induced macrophage antimicrobial activity was investigated by overexpressing hsa-mir-21 expression during *M. tuberculosis* infection.

For these experiments the avirulent *M. tuberculosis* H37Ra strain was used since it does not contain a PGL-I homologue and failed to induce expression of hsa-mir-21 in monocytes upon infection (Supplemental Fig. 10a), despite induction of IL-6 mRNA in the same cells (Supplemental Fig. 10b). Monocytes were transfected with hsa-mir-21 or a control oligo, then infected with *M. tuberculosis* H37Ra overnight, subsequently treated with the TLR2/1 ligand for 3 d and bacterial viability assessed by qPCR according to the ratio of 16S RNA to IS6110 DNA [10]. TLR2/1L induced an antimicrobial activity against *M. tuberculosis* in monocytes transfected with a control oligo (Fig. 6a), at a level consistent with previous studies using the standard CFU assay [6]. However, overexpression of hsa-mir-21 blocked the antimicrobial response and resulted in an increase of *M. tuberculosis* viability in TLR2/1L activated cells (Fig. 6a). Also, in unstimulated cells, hsa-mir-21 increased bacterial viability. Overall, *M. tuberculosis* viability in TLR2/1L-treated as compared to control monocytes was significantly higher in the presence of hsa-mir-21 ($P = 0.01$, Fig. 6b).

To address the role of *M. leprae*-induced hsa-mir-21 in regulation of TLR2/1-induced antimicrobial activity, monocytes were transfected with αmir-21 or αmir-neg, then infected with live *M. leprae*. The transfected and infected cells were treated with the TLR2/1L for 3 d and antimicrobial activity assessed by qPCR by measuring the ratio of 16S RNA to RLEP DNA [10]. In αmir-neg transfected cells, TLR2/1-activation increased bacterial viability, consistent with previous findings indicating enhanced *M. tuberculosis* growth in TLR2/1-stimulated cells in the absence of *CAMP* and *DEFB4A* [6]. Strikingly, in αmir-21 transfected monocytes, TLR2/1-activation resulted in decreased bacterial viability (Fig. 6c). The αmir-21 oligo had no effect on *M. leprae* viability in unstimulated monocytes (Fig. 6c). In five donors tested, *M. leprae* viability in TLR2/1-stimulated cells was significantly lower in the presence of αmir-21 ($P = 0.02$, Fig. 6d). Together, the data from these infection experiments demonstrate the biologic relevance of hsa-mir-21 in innate host defense: the expression of hsa-mir-21 is sufficient to block TLR2/1-induced antimicrobial responses and the silencing of hsa-mir-21 induction restores TLR2/1-mediated antimicrobial activity.

Discussion

Interactions between the pathogen and the host determine the outcome of the immune response to microbial infection. The present data provides evidence that the human pathogen, *M. leprae*, regulates the microRNA profile at the site of infection in subjects with leprosy and interferes with the host antimicrobial response. We employed a novel bioinformatic strategy, combining an enrichment analysis of leprosy disease-type specific miRNA species ranked by 3′UTR mRNA targeting preference and evaluated by the Kolmogorov-Smirnov-based permutation test. Together, this led to the identification of hsa-mir-21 as being differentially expressed in the progressive L-lep form of leprosy with the potential to target genes in the vitamin D antimicrobial pathway. Infection of human monocytes with live *M. leprae,* or treatment with the mycobacterial virulence factor PGL-I, induced expression of hsa-mir-21. Next. hsa-mir-21 was demonstrated to functionally downregulate the TLR2/1-induced vitamin D antimicrobial pathway, by directly targeting *CYP27B1* and IL-1β, as well as the indirect induction of IL-10, all leading to the inhibition of antimicrobial peptides *CAMP* and *DEFB4A*. Silencing of hsa-mir-21 during *M. leprae* infection led to the enhanced expression of vitamin D pathway genes. Finally, introduction

of hsa-mir-21 into monocytes was sufficient to block TLR2/1-induced antimicrobial activity against *M. tuberculosis*, and the silencing of hsa-mir-21 induction restored TLR2/1-mediated antimicrobial activity against *M. leprae*. Therefore, these data identify an evasion strategy, in which a microbial pathogen regulates the host microRNA profile at the site of infection to inhibit the antimicrobial response.

Although *M. leprae* was the first human pathogen discovered [11], it still cannot be grown in the laboratory, providing a major obstacle to investigation of the immunology of leprosy. To our knowledge, it has not been possible to demonstrate immune-mediated antimicrobial activity against *M. leprae* in primary human cells [12]. Comparison of antimicrobial responses in mouse and human macrophages demonstrated that the combination of lipopolysaccharide and interferon-γ reduced the viability of intracellular *M. leprae* in mouse but not human macrophages [12]. Here, we successfully demonstrate that immune activation of *M. leprae*-infected human monocytes decreases bacterial viability, finding that TLR2/1 activation induces a four-fold reduction in *M. leprae* viability only when hsa-mir-21 was silenced. In addition, overexpression of hsa-mir-21 blocked the TLR2/1-induced antimicrobial activity against *M. tuberculosis* resulting in a five-fold increase in bacterial viability. Taken together, these data indicate the biological relevance of hsa-mir-21 in the host antimicrobial response.

Insight into the mechanism by which *M. leprae* induces a specific miRNA immune regulatory profile at the site of infection was revealed by identifying that hsa-mir-21 was induced in monocytes following *M. leprae* infection or by treatment with *M. leprae*-derived PGL-I. Previously, PGL-I has been shown to inhibit monocyte responses [13, 14], as well as associate with mycobacterial virulence [15]. Further studies are needed to elucidate the mechanism of induction and functional role of those microRNAs differentially expressed in L-lep lesions. Given that the degree of genetic diversity in *M. leprae* clinical isolates is not as broad as compared with other human pathogens [16], it is not likely that species subtypes differentially induce single miRNAs as has been shown for *Francisella tularensis* [17]. Complementing the study of miRNA profiles in disease lesions as shown here, additional insight can be obtained by profiling the miRNAs induced by a pathogen in an isolated cell type [18]. It should be possible to learn whether the ability of a pathogen to induce a single or set of miRNA species that targets and inhibits host immune responses provides a potential virulence mechanism that contributes to the pathogenesis of infectious disease [19].

Our data demonstrate that a single miRNA species, by both directly and indirectly regulating immune modulatory genes, can affect the downstream effectors of an innate immune triggered antimicrobial pathway. Specifically, hsa-mir-21 inhibited TLR-induced *CYP27B1* and *IL1B* gene expression, as well as enhanced IL-10 expression, thereby preventing upregulation of the CAMP and DEFB4 mRNAs which encode antimicrobial peptides. These factors are all key to the outcome of the vitamin D antimicrobial pathway: i) CYP27b1 converts inactive to active vitamin D leading to antimicrobial activity, ii) IL-1β is required for DEFB4 induction, and iii) IL-10 is known to inhibit TLR-induced responses [20]. Consequently, hsa-mir-21 inhibits the innate immune response by its distinct gene regulatory activities: the indirect upregulation of an immunosuppressive cytokine and direct targeting of epigenetic components required for the TLR-induced, vitamin D dependent antimicrobial pathway [5, 6]. Consistent with this model, the genes directly targeted by hsa-

mir-21, *CYP27B1* and *IL1B* are downregulated in L-lep vs. T-lep lesions [2, 4]. Although the expression of microRNAs and gene targets in disease lesions is correlative, the demonstration that hsa-mir-21 is induced in human primary monocytes 18 h after *M. leprae* infection and its effect on the TLR-induced antimicrobial response suggests a role in disease pathogenesis. The investigation of the effect of a single miRNA in leprosy provides a framework for analyzing the set of miRNAs that are differentially expressed at the site of disease to determine their cumulative role in regulating the host immune response, including autophagy and antimicrobial pathways.

The ability of αmir-21 to enhance the vitamin D-dependent antimicrobial pathway provides a potential therapeutic strategy to intervene in human infectious disease. In leprosy, the vitamin D antimicrobial pathway may contribute to disease outcome based upon: i) the preferential expression of antimicrobial pathway genes in the T-lep vs. L-lep form [4], ii) the correlation of VDR single nucleotide polymorphism in L-lep subjects [21]; and, iii) the reported successful use of vitamin D as a therapeutic adjuvant in the treatment of leprosy [22]. Potentially, the combination of vitamin D supplementation with miRNA targeted therapy could provide an optimal treatment approach to leprosy and other chronic infectious diseases in which the cellular immune response is dysregulated. This type of approach may be particularly worth exploring in the clinical setting of drug resistant pathogens including MDR, XDR and TDR (totally drug resistant) tuberculosis, in which antimicrobial therapy is becoming increasingly problematic. Finally, our findings may be relevant to other diseases including infectious [23, 24], autoimmune [25] and neoplastic [26, 27], in which vitamin D sufficiency has been shown to be required for optimal host immunity.

METHODS

Statistical analysis

Percent change due to miRNA or antagomir were analyzed against no change using an unpaired Student's *t*-test. Gene or miRNA induction studies were analyzed using an unpaired Student's *t*-test against the medium control of each experiment. L-lep specific miRNA targeting of Th1- and Th2- related genes was analyzed using an unpaired Student's *t*-test. The miRNA targeting preference was determined using the Kolmogorov-Smirnov (KS)-based permutation analysis as noted in the Supplemental Text. Error bars represent the standard error between individual donor values.

Leprosy biopsy specimens

The acquisition of all specimens was approved by the committees on investigations involving human subjects of the University of California, Los Angeles, more details can be found in the Supplemental Methods. Scalpel or punch skin biopsy specimens were obtained after informed consent from patients with tuberculoid leprosy and patients with lepromatous leprosy at the time of diagnosis; therefore, all samples are representative of untreated disease.

Microarray analysis

For gene and miRNA expression profiling, the RNA from skin biopsy specimens were processed and analyzed by the UCLA Clinical Microarray Core Facility using the Affymetrix U133 Genechip and Asuragen using the Discovarray platform, respectively. Additional details pertaining hierarchical clustering, cluster dendrograms, and heatmaps are included in the Supplemental Methods.

In situ hybridization

Leprosy skin biopsy specimens were snap frozen and sectioned to a thickness of 10 μm, and then mounted onto a glass slide. The protocol has been previously described [28] and adapted for current use. Briefly, biotinylated hsa-mir-21 specific, U6 and non-specific control probes were purchased (Exiqon) and were hybridized to the tissue at 0.1 pg μl^{-1} for 1–4 h followed by incubation with streptavidin-horseradish peroxidase (*S*A-HRP). Then, the sections were incubated with the TSA^{TM} Plus Fluorescein System (Perkin Elmer) according to the manufacturer's instructions. A coverslip was sealed to the slides with ProLong® Gold with DAPI (Invitrogen), left to dry at 4°C in the dark overnight, and imaged using a Leica FLIM confocal microscope (Leica).

Live M. leprae

Live and viable *M. leprae* bacteria were generously donated by Dr. James L. Krahenbuhl of US National Hansen's Disease Programs, Health Resources Service Administration, Baton Rouge, LA. Additional information is included in the Supplemental Methods.

Quantitative PCR

For miRNA analysis, qPCR was performed using the TaqMan® MicroRNA Cells-to-CT kit in conjunction with the TaqMan® MicroRNA Assay for hsa-mir-21 (Applied Biosystems) or the NCODE miRNA cDNA Synthesis and qPCR Kit (Invitrogen) according to the manufacturers' recommended conditions. For mRNA studies, total RNA was isolated from monocytes by TRIzol® (Invitrogen), and cDNA libraries were made using the iScript cDNA synthesis kit (BioRAD). qPCR reactions were carried out using the iQ SYBR Green qPCR Master Mix (BioRAD) according to the manufacturers recommended conditions. The primer sequences for h36B4, CAMP, DEFB4, and CYP27B1 were previously published [5, 6], other primer sequences and calculations are included in the Supplemental Methods.

Transfection of monocytes

Monocytes were enriched from PBMCs using a Percoll (GE Healthcare) gradient as previously described [6], and then transfected with either the mature miRNA the antagomir oligos using the Amaxa Nucleofector system with the Human Monocyte Nucleofector transfection kit (Lonza) according to the manufacturer's recommended protocol. Additional details are included in the Supplemental Methods.

miRNA Direct Targeting Analysis

MiRNA targeting plasmids were prepared with endotoxin free conditions using the Qiagen Endofree Maxi Kit (Qiagen) according to the manufacturer's recommended protocols. The

constructs were co-transfected into HEK-293 cells with either hsa-mir-21 mature oligo or a non-targeting control oligo using the Amaxa Nucleofector Transfection Cell Line V kit (Lonza) according to the manufacturer's optimized protocol. Following transfection the cells are rested for 2 h and then washed to replace the medium. The transfected cells are then incubated 37°C for 16 h and then luciferase activity was measured using the Dual Glo-Luciferase Assay System (Promega) according to the manufacturer's recommended protocols. The miRNA effect is calculated as a ratio of the fire fly to renilla luciferase activities.

Antimicrobial assays

In order to assess *M. leprae* and *M. tuberculosis* H37Ra viability from infected macrophages, we adapted the previously described real time PCR based method for the assessment of bacterial viability, which compares 16S RNA levels to a genomic DNA levels as a predictor of bacterial viability (Supplemental Text) [10]. Experimental details are included in the Supplemental Methods. The 16S and bacterial DNA values were calculated using the C_T analysis, with the bacterial DNA value serving as the housekeeping gene. The *M. leprae* 16S and *M. leprae* repetitive genomic element (RLEP) primers used were as previously described [10], other primer sequences are included in Supplementary Methods.

Other methods

Other methods, including reagent information, can be found in the Supplemental Methods.

Supplementary Material

Refer to Web version on PubMed Central for supplementary material.

Acknowledgments

References

1. Ridley DS, Jopling WH. Classification of leprosy according to immunity. A five-group system. Int J Lepr. 1966; 34:255–273.

2. Yamamura M, et al. Defining protective responses to pathogens: cytokine profiles in leprosy lesions. Science. 1991; 254:277–279. [PubMed: 1925582]

3. Salgame P, et al. Differing lymphokine profiles of functional subsets of human CD4 and CD8 T cell clones. Science. 1991; 254:279–282. [PubMed: 1681588]

4. Montoya D, et al. Divergence of macrophage phagocytic and antimicrobial programs in leprosy. Cell Host Microbe. 2009; 6:343–353. [PubMed: 19837374]

5. Liu PT, et al. Toll-like receptor triggering of a vitamin D-mediated human antimicrobial response. Science. 2006; 311:1770–1773. [PubMed: 16497887]

6. Liu PT, et al. Convergence of IL-1beta and VDR activation pathways in human TLR2/1-induced antimicrobial responses. PLoS ONE. 2009; 4:e5810. [PubMed: 19503839]

7. Lu TX, Munitz A, Rothenberg ME. MicroRNA-21 is up-regulated in allergic airway inflammation and regulates IL-12p35 expression. J Immunol. 2009; 182:4994–5002. [PubMed: 19342679]

8. Sheedy FJ, et al. Negative regulation of TLR4 via targeting of the proinflammatory tumor suppressor PDCD4 by the microRNA miR-21. Nat Immunol. 2010; 11:141–147. [PubMed: 19946272]

9. Adams LB, et al. The study of Mycobacterium leprae infection in interferon-gamma gene--disrupted mice as a model to explore the immunopathologic spectrum of leprosy. J Infect Dis. 2002; 185(Suppl 1):S1–8. S1–S8. [PubMed: 11865434]

10. Martinez AN, et al. Molecular determination of Mycobacterium leprae viability by use of real-time PCR. J Clin Microbiol. 2009; 47:2124–2130. [PubMed: 19439537]

11. Hansen GA. Undwersogelser angaende spedalskhedens arsager. Norsk Mag Laegevid. 1874; 4:1–88.

12. Pena MT, et al. Expression and characterization of recombinant interferon gamma (IFN-gamma) from the nine-banded armadillo (Dasypus novemcinctus) and its effect on Mycobacterium leprae-infected macrophages. Cytokine. 2008; 43:124–131. [PubMed: 18558493]

13. Vachula M, Holzer TJ, Andersen BR. Suppression of monocyte oxidative response by phenolic glycolipid I of Mycobacterium leprae. J Immunol. 1989; 142:1696–1701. [PubMed: 2537362]

14. Neill MA, Klebanoff SJ. The effect of phenolic glycolipid-1 from Mycobacterium leprae on the antimicrobial activity of human macrophages. J Exp Med. 1988; 167:30–42. [PubMed: 2826638]

15. Tabouret G, et al. Mycobacterium leprae phenolglycolipid-1 expressed by engineered M. bovis BCG modulates early interaction with human phagocytes. PLoS Pathog. 2010; 6:e1001159. [PubMed: 20975946]

16. Clark-Curtiss JE, Walsh GP. Conservation of genomic sequences among isolates of Mycobacterium leprae. J Bacteriol. 1989; 171:4844–4851. [PubMed: 2570057]

17. Cremer TJ, et al. MiR-155 induction by F. novicida but not the virulent F. tularensis results in SHIP down-regulation and enhanced pro-inflammatory cytokine response. PLoS ONE. 2009; 4:e8508. [PubMed: 20041145]

18. Liu Z, et al. Up-regulated microRNA-146a negatively modulate Helicobacter pylori-induced inflammatory response in human gastric epithelial cells. Microbes Infect. 2010; 12:854–863. [PubMed: 20542134]

19. Sinsimer D, et al. Mycobacterium leprae actively modulates the cytokine response in naive human monocytes. Infect Immun. 2010; 78:293–300. [PubMed: 19841079]

20. Krutzik SR, et al. Activation and regulation of Toll-like receptors 2 and 1 in human leprosy. Nat Med. 2003; 9:525–532. [PubMed: 12692544]

21. Roy S, et al. Association of vitamin D receptor genotype with leprosy type. J Infect Dis. 1999; 179:187–191. [PubMed: 9841838]

22. HERRERA G. Vitamin D in massive doses as an adjuvant to the sulfones in the treatment of tuberculoid leprosy. Int J Lepr. 1949; 17:35–42. [PubMed: 18143438]

23. Rook GAW. The role of vitamin D in tuberculosis. Am Rev Resp Dis. 1988; 138:768–770. [PubMed: 2849343]

24. Crowle AJ, Ross EJ, May MH. Inhibition by 1,25(OH)2-vitamin D3 of the multiplication of virulent tubercle bacilli in cultured human macrophages. Infect Immun. 1987; 55:2945–2950. [PubMed: 3119492]

25. Munger KL, Levin LI, Hollis BW, Howard NS, Ascherio A. Serum 25-hydroxyvitamin D levels and risk of multiple sclerosis. JAMA. 2006; 296:2832–2838. [PubMed: 17179460]

26. Lappe JM, Travers-Gustafson D, Davies KM, Recker RR, Heaney RP. Vitamin D and calcium supplementation reduces cancer risk: results of a randomized trial. Am J Clin Nutr. 2007; 85:1586–1591. [PubMed: 17556697]

27. Ahn J, et al. Vitamin D-related genes, serum vitamin D concentrations and prostate cancer risk. Carcinogenesis. 2009; 30:769–776. [PubMed: 19255064]

28. Silahtaroglu AN, et al. Detection of microRNAs in frozen tissue sections by fluorescence in situ hybridization using locked nucleic acid probes and tyramide signal amplification. Nat Protoc. 2007; 2:2520–2528. [PubMed: 17947994]

AUTHOR CONTRIBUTIONS

ACCESSION NUMBERS

Gene	NCBI Accession
CAMP	NM_004345
DEFB4A	NM_004942
CYP27B1	NM_000785
IL1B	NM_000576
IL6	NM_000600
IL10	NM_000572
IL12A	NM_000882
IL12B	NM_002187
36B4	NM_001002

miRNA	miRBase Accession
hsa-mir-21	MI0000077
hsa-let-7c	MI0000064

mRNA Array (GEO Title)	GEO Accession
T-lep1 (BT1)	GSM443590
T-lep2 (BT6)	GSM443591
T-lep3 (BT10)	GSM443678
T-lep4 (BT3)	GSM443592
T-lep5 (BT4)	GSM443622
T-lep6 (BT7)	GSM443625
L-lep1 (LL1)	GSM443583
L-lep2 (LL4)	GSM443586
L-lep4 (LL3)	GSM443585
L-lep5 (LL7)	GSM443588
L-lep6 (LL9)	GSM443589

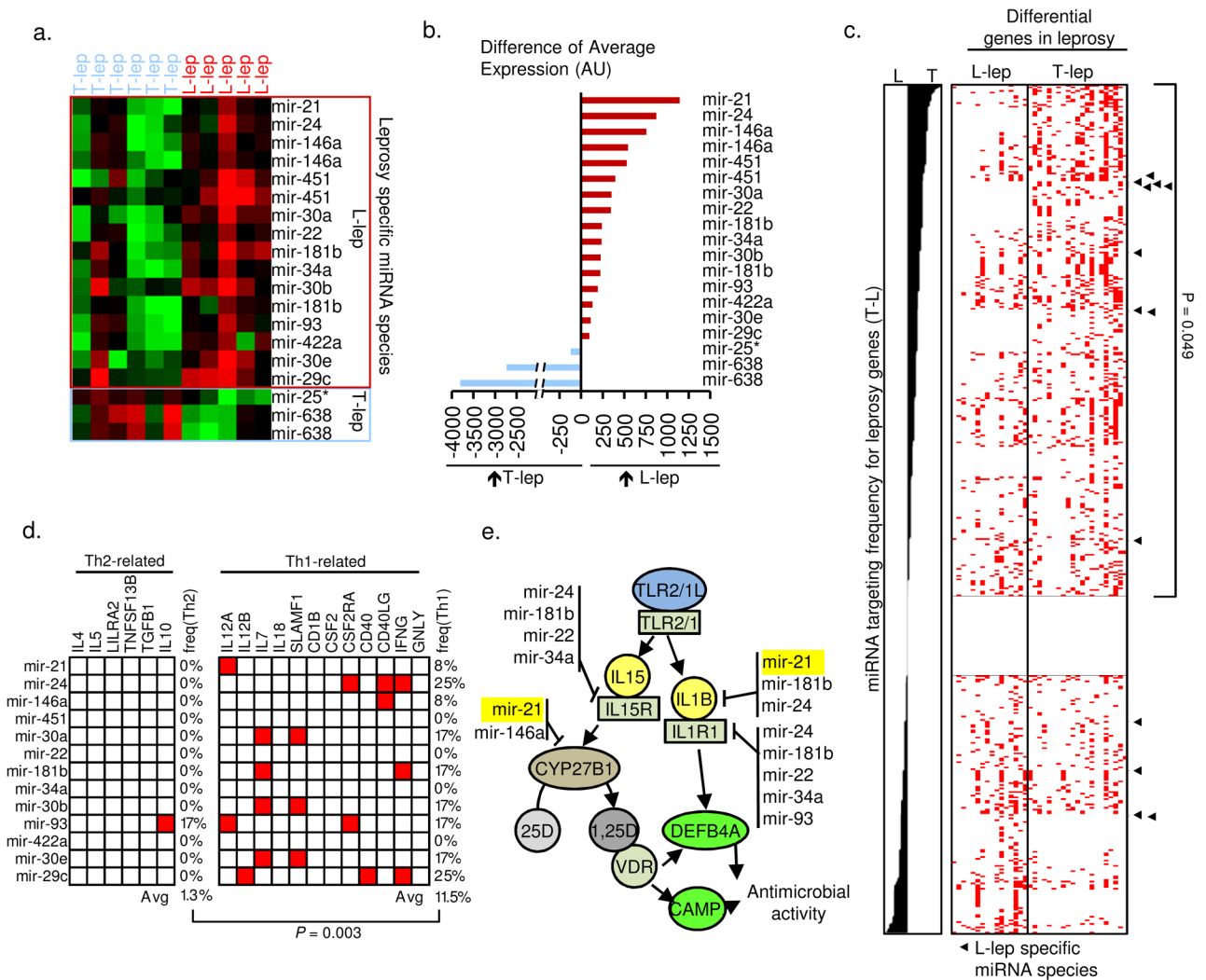| miRNA Array	GEO Acession
T-lep1	GSM821609
T-lep2	GSM821610
T-lep3	GSM821611
T-lep4	GSM821612
T-lep5	GSM821613
T-lep6	GSM821614
L-lep1	GSM821604
L-lep2	GSM821605
L-lep4	GSM821606
L-lep5	GSM821607
L-lep6	GSM821608
Study	GSE33192

Figure 1.
MiRNA expression and targeting profile in leprosy. MiRNA probes that are differentially expressed between T-lep and L-lep lesions displayed as (**a**) normalized data and (**b**) raw expression values. (**c**) All miRNA species represented on the microarray platform ranged by targeting preference score. ◄ = L-lep specific miRNA species. (**d**) Targeting preference of the L-lep or T-lep specific miRNA species for Th2- or Th1-related genes. Red box represents a predicted target site within the 3′UTR of the indicated gene. (**e**) L-lep specific miRNA species and predicted targeting of genes in the TLR-induced vitamin D-dependent antimicrobial pathway.
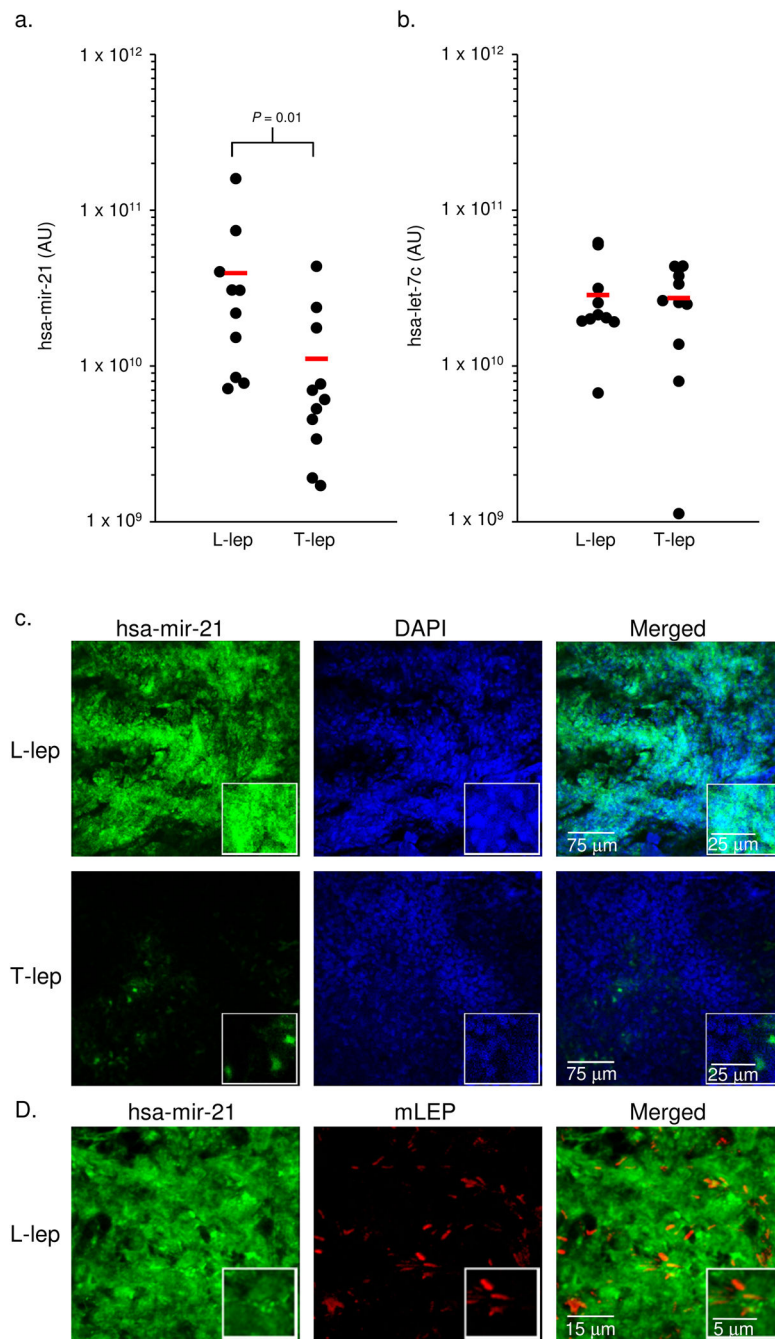
Figure 2.
Expression of hsa-mir-21 in leprosy. Expression levels of (**a**) hsa-mir-21 and (**b**) hsa-let-7c comparing L-lep vs. T-lep lesions by qPCR. The levels of hsa-mir-21 and hsa-let-7c are normalized to 36B4 levels in the same tissue and displayed as values from individual lesions (●) as well as the average (–) of 10 L-lep lesions and 11 T-lep lesions. (**c**) Skin biopsy sections from L-lep or T-lep subjects were probed with a hsa-mir-21 specific oligo using fluorescent *in situ* hybridization. Cellular nuclei were visualized using DAPI. Data shown is representative experiment for four individual L-lep samples and three individual T-lep

samples. (**d**) Skin biopsy section derived from L-lep subjects were probed for hsa-mir-21 and *M. leprae* using fluorescent *in situ* hybridization in conjunction with a monoclonal antibody specific for *M. leprae*, detected by confocal microscopy. Data shown is representative experiment from three individual subjects.
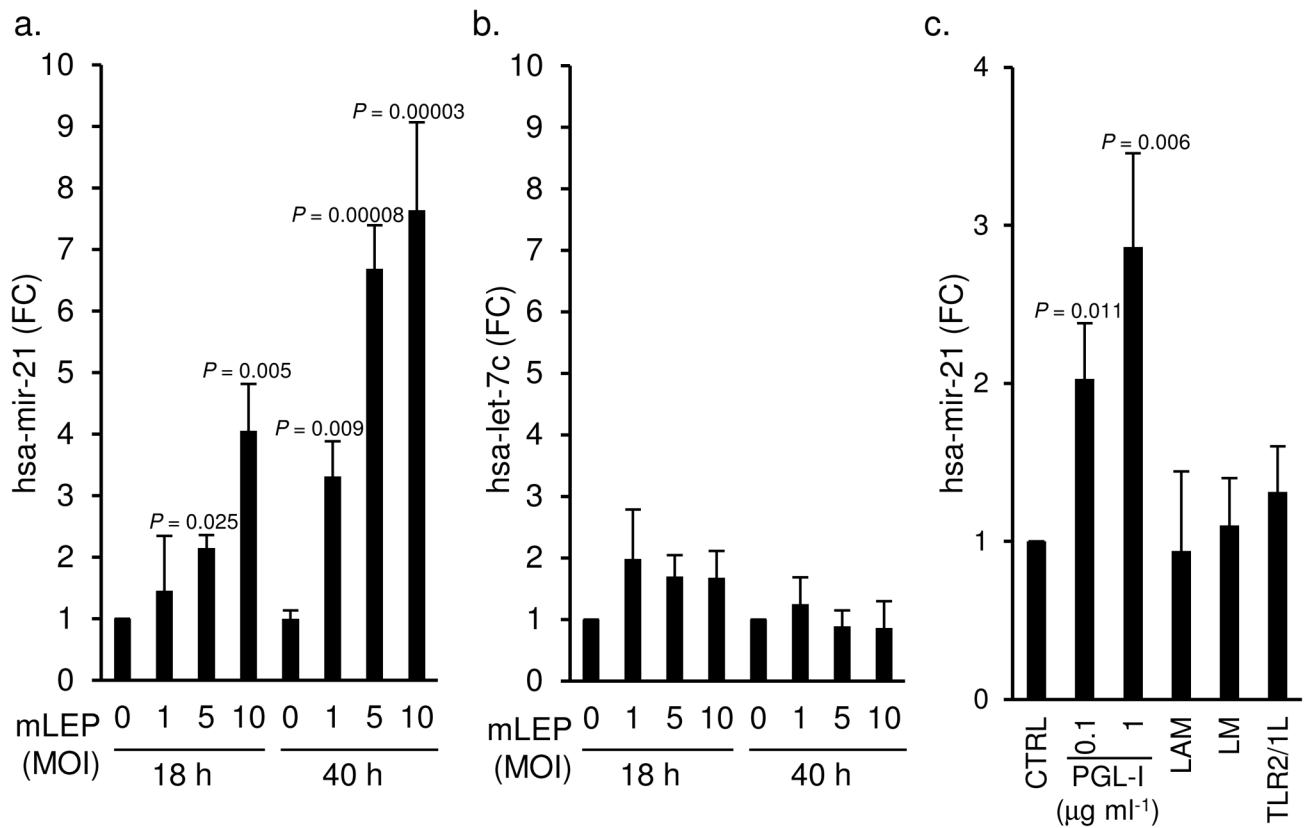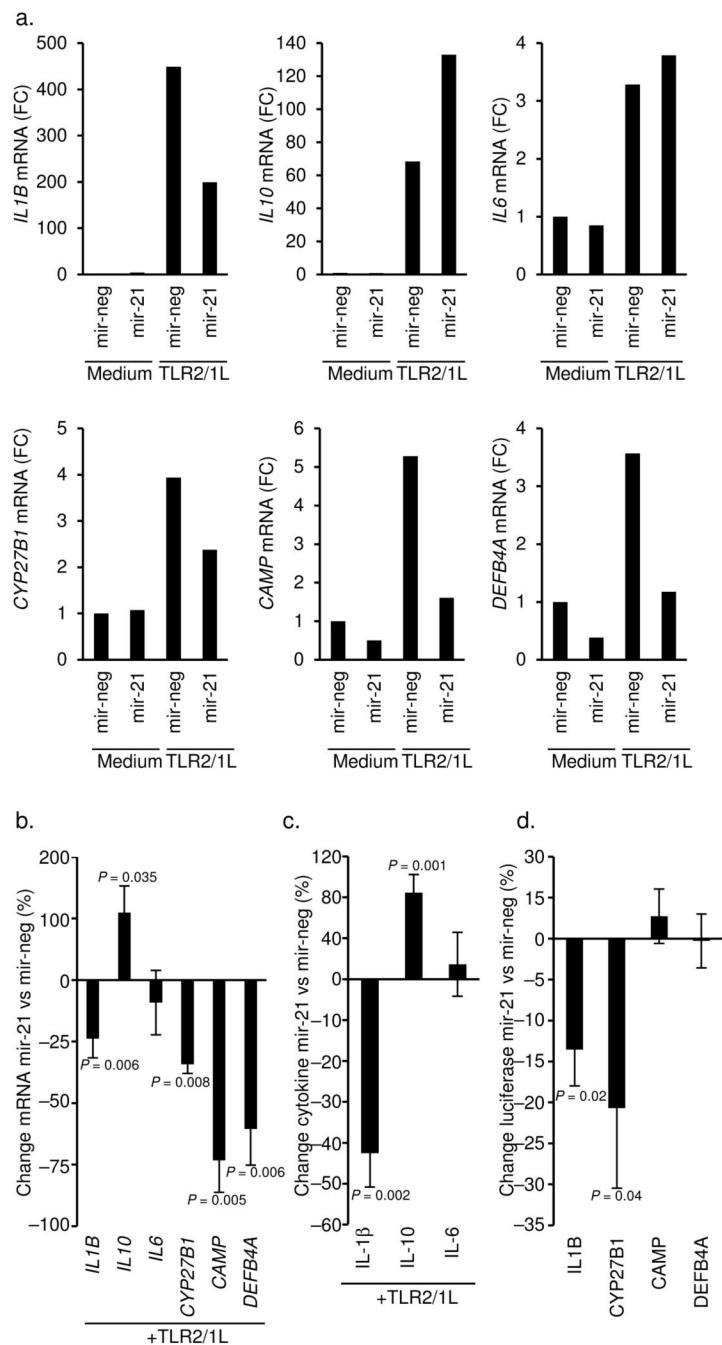
Figure 3.
Regulation of hsa-mir-21 levels in primary human monocytes by *M. leprae*. Levels of (**a**) hsa-mir-21 and (**b**) hsa-let-7c in primary human monocytes infected with *M. leprae* at MOI of 0, 1, 5, and 10 for 18h and 40h. Data shown is mean of fold change compared to no infection control ± SEM, *n* = 3–5. Levels of hsa-mir-21 (**c**) in primary human monocytes after treatment with PGL-I, LAM (10μg ml^{-1}), LM (10μg ml^{-1}), and TLR2/1L for 18 h. Data shown is mean fold change compared to the vehicle control treated cells ± SEM, *n* = 3–10.

Figure 4.
The ability of hsa-mir-21 to regulate the innate immune response in human monocytes.
Primary human monocytes were transfected with the mature hsa-mir-21 (mir-21) oligo or a
non-targeting control (mir-neg) then treated with TLR2/1L for 18 h and 24 h. Gene
expression of (**a**) *IL1B* at 18 h, *IL10* at 24 h, *IL6* at 16 h, *CYP27B1* at 16 h, *CAMP* at 24 h
and *DEBF4A* at 24 h, were evaluated by qPCR. Data shown are representative experiments
from greater than five individual donors. (**b**) Change in gene expression comparing mir-21
to mir-neg transfected cells following TLR2/1L simulation. Data shown is average percent

change mir-21 vs mir-neg ± SEM, n = 3–11 (**c**) Change in cytokine protein levels in culture supernatants comparing mir-21 to mir-neg transfected cells following TLR2/1L stimulation. Data shown in average percent change mir-21 vs mir-neg ± SEM, n = 4–6. Representative experiment is shown in Supplemental Fig. 6. (**d**) Change in luciferase activity of cells co-transfected with a 3′UTR luciferase reporter construct (*IL1B, CYP27B1, CAMP, DEFB4A*) and either mir-21 or mir-neg. Data shown is mean percent change of each individual 3′UTR construct comparing mir-21 vs mir-neg ± SEM, n = 4–6. Representative experiment is shown in Supplemental Fig. 8.
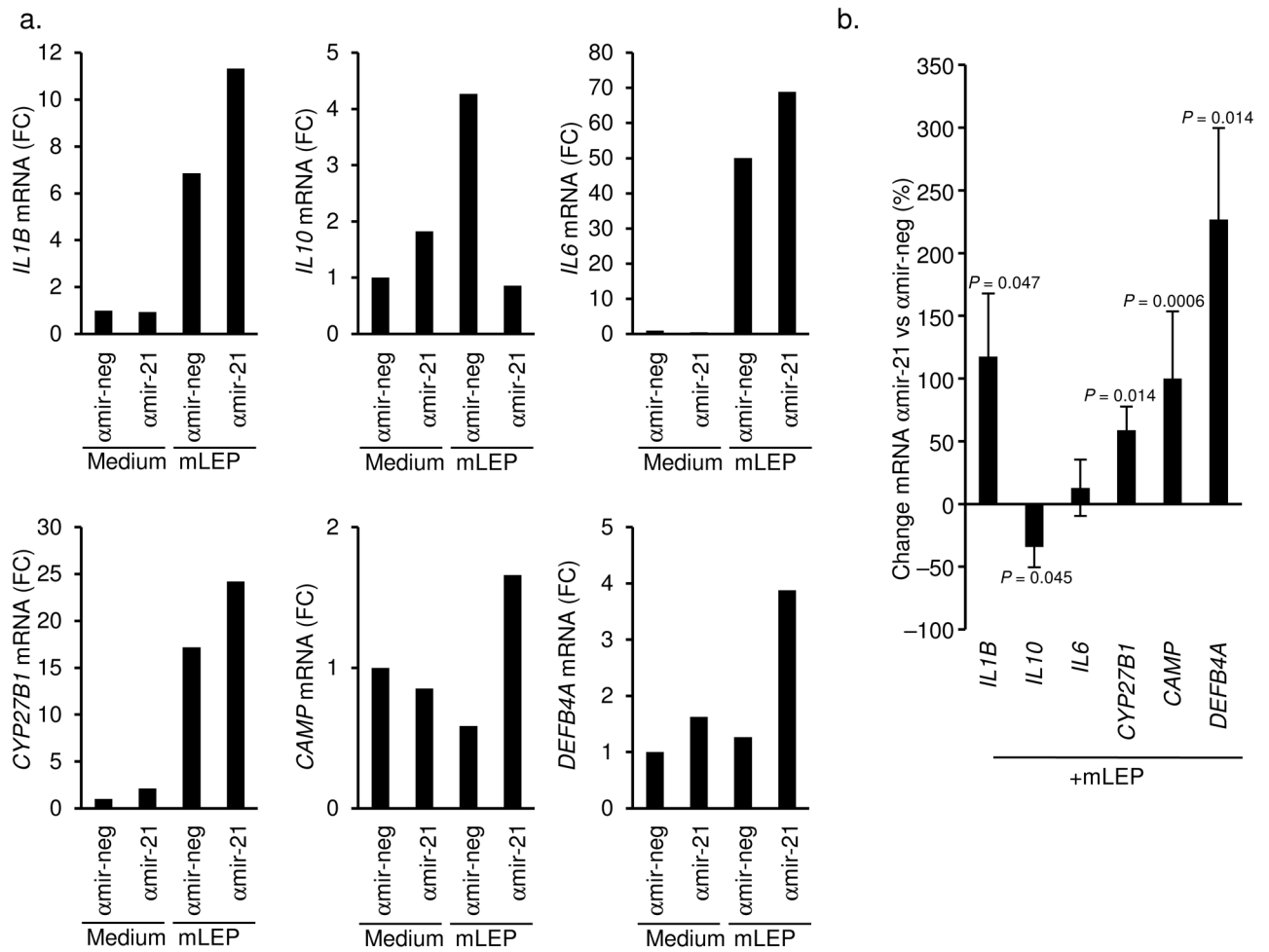
Figure 5.
Role of hsa-mir-21 expression during *M. leprae* infection. Primary human monocytes were transfected with the antagomir against hsa-mir-21 (αmir-21) oligo or a non-specific control (αmir-neg) then infected with live *M. leprae* at an MOI of 10 for 18 h. Gene expression of *IL1B*, *IL10*, *IL6*, *CYP27B1*, *CAMP* and *DEFB4A* were evaluated by qPCR. Data shown (**a**) are representative experiments from greater than four individual donors. (**b**) Change in gene expression comparing αmir-21 to αmir-neg transfected cells following *M. leprae* infection for 18 h. Data shown is average percent change αmir-21 vs. αmir-neg ± SEM, $n = 4$–8.
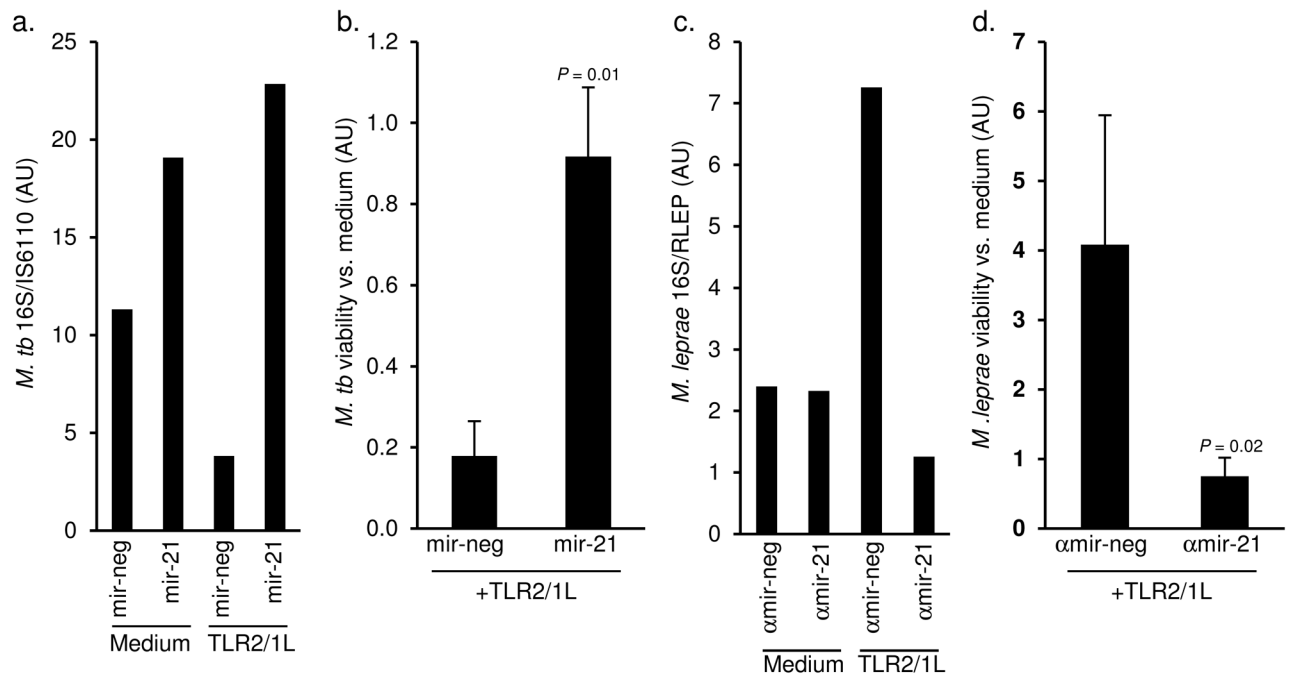
Figure 6.
Role of hsa-mir-21 in TLR2/1-mediated antimicrobial activity. Primary human monocytes were transfected with the mature hsa-mir-21 (mir-21) oligo or a non-targeting control (mir-neg) then infected with live *M. tuberculosis* H37Ra at an MOI of 0.5 for 18 h. The monocytes were then treated with the TLR2/1L ($10\mu g\ ml^{-1}$) for 3 d. Levels of 16S rRNA and IS6110 DNA levels were assessed by qPCR. Data shown is the ratio of 16S rRNA to IS6110 DNA levels as (**a**) a representative experiment from three donors. (**b**) Fold change in *M. tuberculosis* viability comparing TLR2/1L vs. medium treated monocytes. Data shown is the mean fold change ± SEM, *n* = 3. Primary human monocytes were transfected with the antagomir against hsa-mir-21 (αmir-21) oligo or a non-specific control (αmir-neg) then infected with live *M. leprae* at an MOI of 10 for 18 h. The monocytes were then treated with the TLR2/1L ($10\mu g\ ml^{-1}$) for 3 d. Levels of 16S rRNA and RLEP DNA levels were assessed by qPCR. Data shown is the ratio of 16S rRNA to RLEP DNA levels as (**c**) a representative experiment from five donors. (**d**) Fold change in *M. leprae* viability comparing TLR2/1L vs. medium treated monocytes. Data shown is the mean fold change ± SEM, *n* = 5.